Weierstraß-Institut
für Angewandte Analysis und Stochastik

Leibniz-Institut im Forschungsverbund Berlin e. V.

Preprint ISSN 2198-5855

Temporal dissipative solitons in the Morris–Lecar model with time-delayed feedback

Mina Stöhr, Matthias Wolfrum

submitted: November 16, 2022

Weierstrass Institute
Mohrenstr. 39
10117 Berlin
Germany
E-Mail: mina.stoehr@wias-berlin.de
matthias.wolfrum@wias-berlin.de

No. 2970
Berlin 2022

2020 *Mathematics Subject Classification.* 34K16, 34K26.

Key words and phrases. Temporal dissipative solitons, time-delayed feedback, homoclinic orbit flip.

The authors acknowledge helpful discussions with S. Ruschel and S. Yanchuk.
This work was supported by the Deutsche Forschungsgemeinschaft (DFG) within the framework of the SFB 910 - Project number 163436311.

Edited by
Weierstraß-Institut für Angewandte Analysis und Stochastik (WIAS)
Leibniz-Institut im Forschungsverbund Berlin e. V.
Mohrenstraße 39
10117 Berlin
Germany

Fax: +49 30 20372-303
E-Mail: preprint@wias-berlin.de
World Wide Web: http://www.wias-berlin.de/

Temporal dissipative solitons in the Morris–Lecar model with time-delayed feedback

Mina Stöhr, Matthias Wolfrum

ABSTRACT. We study the dynamics and bifurcations of temporal dissipative solitons in an excitable system under time-delayed feedback. As a prototypical model displaying different types of excitability we use the Morris–Lecar model. In the limit of large delay soliton like solutions of delay-differential equations can be treated as homoclinic solutions of an equation with an advanced argument. Based on this, we use concepts of classical homoclinic bifurcation theory to study different types of pulse solutions and to explain their dependence on the system parameters. In particular, we show, how a homoclinic orbit flip of a single pulse soliton leads to the destabilization of equidistant multi-pulse solutions and to the emergence of stable pulse packages. It turns out that this transition is induced by a heteroclinic orbit flip in the system without feedback, which is related to the excitability properties of the Morris–Lecar model.

The phenomenon of solitons has been of great interest since its first discovery in the first half of the 19th century by John Scott Russel, who observed a solitary water wave in a canal whilst riding alongside. Solitons can be explained as specific solutions in conservative spatially extended systems, where they appear due to a balance between dispersion and nonlinearity. More recently, they play an important role in nonlinear optical fibres. As they preserve their shape and localization even after collisions, they are of great importance for data transmission. Similarly, localized solutions in dissipative systems are often called dissipative solitons. In contrast to conservative systems, soliton like solutions emerge here due to a balance between energy gain and loss. This can happen not only in optically active material, but also in chemical, biological, or neuronal systems. In some cases, e.g. in certain optoelectronic systems with a time-delayed signal resulting from a cavity round-trip, such localized states can be found also in systems of delay-differential equations where no spatial variable is present and the localization happens in the time variable. In such cases one speaks about temporal dissipative solitons. We investigate in detail the emergence, stability and bifurcations of such solutions in the Morris–Lecar model with time-delayed feedback.

Temporal dissipative solitons (TDSs) are localized states in systems with time delay. Recently, they found application in a variety of fields, particularly in opto- electronic systems. They have been used to describe different types of cavity solitons [9, 12, 34, 38, 39, 28], mode-locked pulses [23, 33, 42], their interaction dynamics [41, 26, 25], and certain specific instabilities [14, 32]. However, a comprehensive mathematical theory for this type of solutions, their instabilities and bifurcations, is still largely absent.

A temporal localization can be observed in situations where the delay time is substantially longer than the internal time scale. In this way there can be solutions that spend most of the time close to a stable background equilibrium except for a short time interval during which the localized structure appears. The localization pattern then repeats with a period slightly larger than the delay time, i.e the soliton is localized within the time window of the delay. This reminds of the analogy of delay-differential equations (DDEs) with large delay and spatially extended systems that has been pointed out already by Politi and Giacomelli in 1996 [10]; for a recent survey, see [43]. The limit of large delay is in fact a singular perturbation and in a natural way induces dynamics on multiple time scales. This has been elaborated in detail for the eigenvalue spectrum of equilibria [20], for the Floquet-spectrum of rapidly oscillating solutions [37], and also for chaotic dynamics [13].

Recently, this approach has been extended to TDSs. It has been shown in [45] that the stability of such solutions is governed by a Floquet-spectrum that is composed by a pseudo-continuous part, accounting for the stability properties of the soliton background, and point spectrum coming from the localized part of the solution. Moreover, it has been pointed out that TDSs can be found as homoclinic solutions of a so called *profile equation*, such that their stability and bifurcations can be described in terms of classical homoclinic bifurcation theory. As the simplest example of a TDS they presented an excitable system with an input from a time-delayed feedback, such that an excitation pulse can replicate itself after a bit more than the delay time and in this way give rise to a periodic appearance of localized pulses. The interaction of solitons in an excitable phase oscillator system has been studied in [25].

In the present paper, we study the Morris–Lecar model with delayed feedback in the excitable regime as an example for more complicated pulse dynamics. In Fig. 1 we show different types of coexisting pulse patterns for different parameter values. There are parameter regions where stable solutions with one or several equidistant pulses coexist (blue trajectories in panels (a), (c), and (d)). Changing a parameter, the equidistant pulses with more than one pulse per delay interval become unstable and stable pulse packages (bursts) appear (purple trajectories in panels (c) and (d)). Changing the parameter further, all the pulse solutions become unstable and a rapidly oscillating solution is the only attractor (red trajectory in panel (c)). Figure 2 shows the corresponding dynamics in space-time representation. In the parameter region of stable equidistant pulses we show a single-pulse soliton in panel (a); an initial condition with two non-equidistant pulses approaches the stable equidistant configuration, see panel (c). In the parameter region of stable pulse packages a similar initial condition tends to the stable two-pulse package, see panel (d). In the region of stable oscillations, an initial condition

DOI 10.20347/WIAS.PREPRINT.2970 Berlin 2022

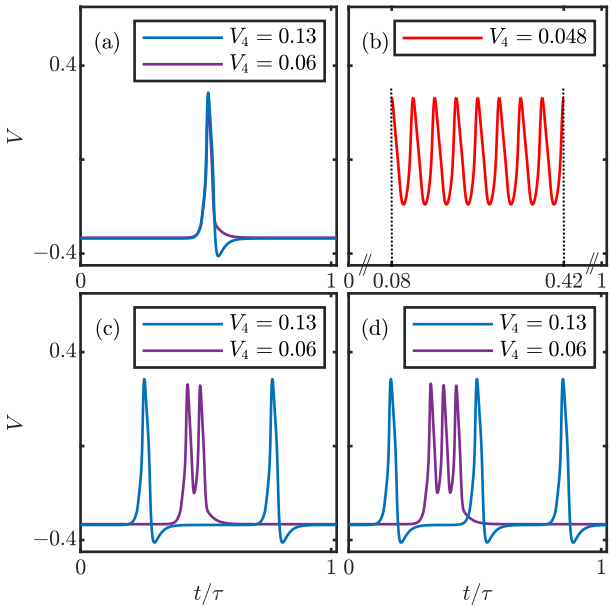

FIGURE 1. Different types of stable periodic solutions of the Morris–Lecar model Eqs. (1a)–(1b) with delayed feedback (5) for different choices of the parameter V_4. At $V_4 = 0.13$ the single pulse soliton coexists with equidistant multi-pulse solutions (blue trajectories). At $V_4 = 0.06$ the single pulse soliton coexists with pulse packages (purple trajectories). At $V_4 = 0.048$ there is only a stable rapid oscillation. Other parameters: $\tau = 100$, $E_l = -0.37$, $\kappa = 0.2$ and as given in Table 1.

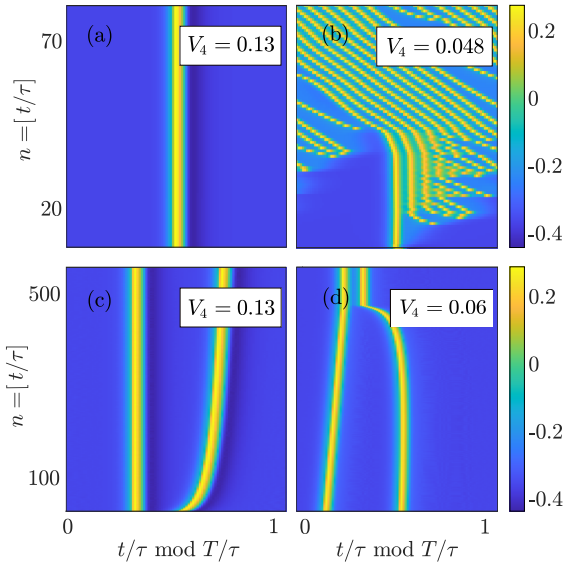

FIGURE 2. Space-time representation of solutions of the Morris–Lecar model Eqs. (1a)–1b with delayed feedback (5). Stable soliton at $V_4 = 0.13$ (a). At $V_4 = 0.13$ a two-pulse solution approaches a stable equidistant configuration (c). At $V_4 = 0.06$ a two-pulse solution approaches a stable pulse package (d). At $V_4 = 0.048$ the single pulse has a trailing edge instability. Parameters: $\tau = 50$, other parameters as in Fig. 1.

with a single pulse develops a trailing-edge instability, which in the course of time leads to the appearance of additional pulses, until the whole delay interval is filled with oscillations, see panel (b).

Our goal is to understand these different feedback induced pulse dynamics in the excitable regime. The paper is organized as follows. First, in section 1, we introduce the Morris–Lecar model and recall some of the bifurcations for the case without feedback. In particular, there is a saddle-node separatrix loop bifurcation, governing the transition between different types of excitability and inducing a heteroclinic orbit flip. Then, in section 2, we introduce the time-delayed feedback and show how it gives rise to TDSs. We recall from [45] how solitons can be found as homoclinic orbits in an equation with advanced

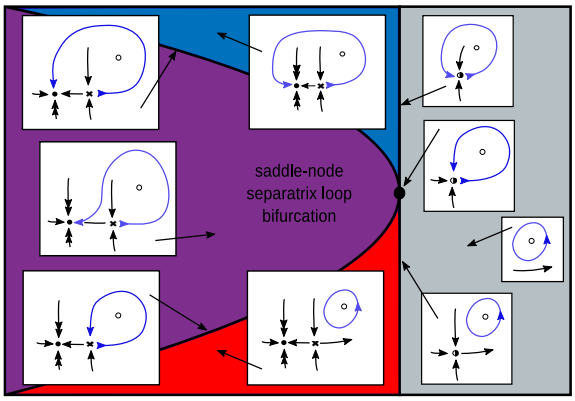

FIGURE 3. Sketch of the unfolding of a saddle-node separatrix loop bifurcation. Coloured parameter regions correspond to different dynamical regimes. Sketched phase portraits in the insets indicate qualitative dynamics in the regions and at the bifurcations.

argument, called *profile equation* and present the stability region of such solutions. We use the software package DDE-biftool [36] for a numerical calculation of all stability boundaries and bifurcations of the TDSs. In section 3, we show how the heteroclinic orbit flip in the system without feedback leads to a homoclinic orbit flip in the profile equation. We then recall how according to classical homoclinic bifurcation theory [15, 35], the homoclinic orbit flip organizes homoclinic orbits with multiple pulses and, in particular organizes the pulse dynamics presented in Fig. 1. In section 4 we conclude with an outlook and discussion of our results.

1. THE MORRIS–LECAR MODEL

The Morris–Lecar model is a model for the dynamics of the action potential in a neuron introduced in [24] given by the two ODEs

$$\dot{V} = I_{ext} - g_l(V - E_l) - g_k w(V - E_k) - g_{Ca} m_\infty(V)(V - E_{Ca}), \tag{1a}$$

$$\dot{w} = \lambda(V)(w_\infty(V) - w), \tag{1b}$$

for the membrane potential V and the recovery variable w. The quantity I_{ext} refers to the applied current stimulus and will be used for the time delayed feedback in section 2. With the voltage dependent sigmoidal activation functions $m_\infty(V)$, $w_\infty(V)$ and the time scale $\lambda(V)$, given as

$$m_\infty(V) = \frac{1}{2}\left(1 + \tanh\left(\frac{V - V_1}{V_2}\right)\right) \tag{2}$$

$$w_\infty(V) = \frac{1}{2}\left(1 + \tanh\left(\frac{V - V_3}{V_4}\right)\right) \tag{3}$$

$$\lambda(V) = \frac{1}{3}\cosh\left(\frac{V - V_3}{2V_4}\right), \tag{4}$$

it is able to reproduce different aspects of neuronal behavior in great detail and has been studied extensively, both from the mathematical [8, 27, 16, 17, 2, 7] and the neuroscientific [24, 22, 40] point of view. In particular, depending on the parameters it can display different types of excitability (Class I and Class II excitablity), which are responsible for the nonlinear response of the system to input signals of different kind [21]. The main underlying mechanism is a codimension-two bifurcation, the so called *saddle-node separatrix loop bifurcation (SNSL)* [31, 5, 6], which we briefly recall below. We use an unfolding of this bifurcation in the parameters V_4 and E_l, while throughout the whole paper we fix all other parameters to the values given in table 1, following Izhikevich[16].

Figure 3 schematically displays the unfolding of a saddle-node separatrix loop bifurcation. The unfolding contains four regions in parameter space with different dynamics. They are separated by three curves of codimension-one bifurcations meeting in the SNSL-point, which is of codimension-two. Within the grey region, there is only one unstable equilibrium and

V_1	V_2	V_3	E_k	E_{Ca}	g_l	g_k	g_{Ca}
0	0.15	0.1	-0.7	1	0.5	2	1.2

TABLE 1. Parameters for the Morris–Lecar model (cf. Izikevich [16])

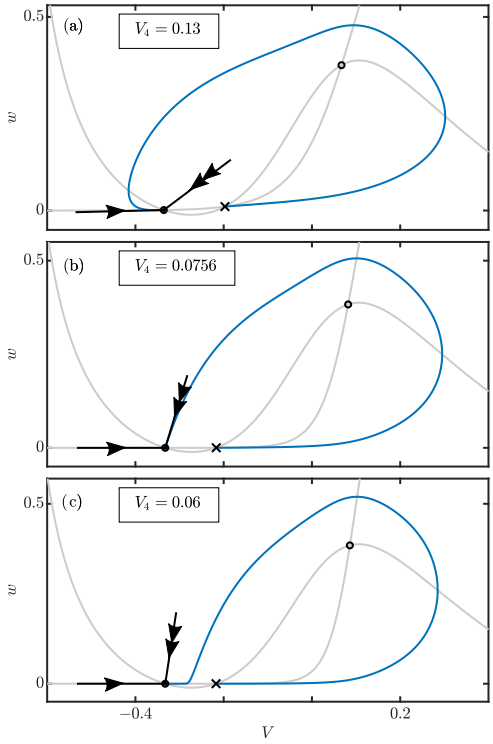

FIGURE 4. Phase portraits of heteroclinic orbits (blue) for the system without feedback $\kappa = 0$. The different choices of parameter V_4 in panels (a)–(c) represent the situation before, directly at, and after the orbit flip, respectivley. Grey lines: nullclines of Eqs. (1a)–(1b). Stable, saddle and unstable equilibrium are indicated by black dot, cross, and circle, respectively. Leading stable eigendirection of stable equilibrium indicated with one arrow, strong stable eigendirection with two arrows. Other parameters as in Fig. 1.

a stable periodic orbit. At the vertical saddle-node curve, separating this region from the other regions, there emerge two more equilibria. In the upper part above the SNSL point it is a saddle-node on invariant circle (SNIC) bifurcation, such that in the blue region the stable equilibrium and the saddle lie on an invariant circle while the periodic orbit has disappeared. Instead, there are two heteroclinic orbits linking the saddle with the stable equilibrium. In the lower part below the SNSL point, the two new equilibria emerge outside the periodic orbit such that in the red region we have a bistable situation with a coexisting stable equilibrium and a periodic orbit. However, passing over to the purple region, the periodic orbit disappears in a homoclinic bifurcation.

At the transition from the purple to the blue region there is a so called *heteroclinic orbit flip*. In Fig. 4 we show in panels (a)–(c) numerically calculated heteroclinic orbits before, directly at, and after this bifurcation. An orbit flip is characterized by the fact that a connecting orbit, which generically approaches the equilibrium along the leading stable eigenvector (single arrows in Fig. 4), switches to the other side and, at the bifurcation, lies in the strong stable subspace (double arrows in Fig. 4).

We focus here on the region with an excitable equilibrium to the left of the saddle-node bifurcation branch and show how the addition of a time-delayed feedback leads to different types of solitons in this region.

2. SOLITONS IN MORRIS–LECAR MODEL WITH TIME-DELAYED FEEDBACK

Adding a time-delayed feedback in the excitable region of the ODE Morris–Lecar model, we expect the creation of soliton solutions. We use a feedback of Pyragas type of the form

$$I_{ext} = \kappa(V(t-\tau) - V(t)), \tag{5}$$

where the delay $\tau > 0$ is chosen substantially bigger than the duration of a pulse and κ denotes the coupling strength. For the rest of the paper, we fix in our calculations $\kappa = 0.2$. While I_{ext} remains small, the DDE dynamics are similar to the ODE dynamics. In particular, for small κ the stability properties of the fixed points do not change qualitatively, such that close to the saddle-node bifurcation we still have two nearby equilibria of stable and saddle type. Note, however, that due to the infinite dimensional phase space of a DDE, there are additionally infintely many stable eigenvalues.

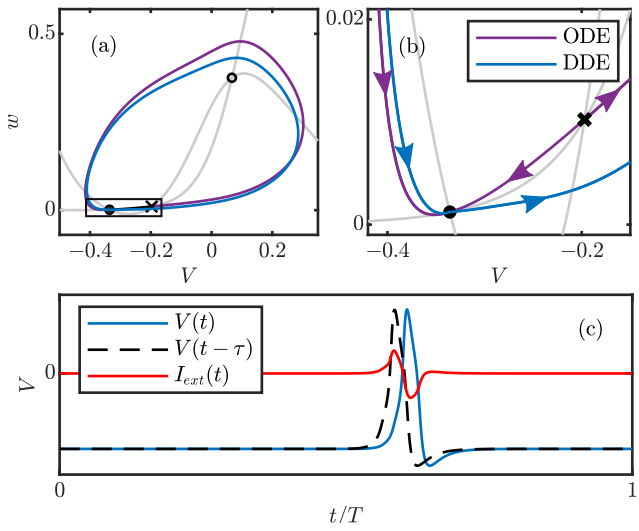

FIGURE 5. (a) – Phase portrait of a soliton solution at $\kappa = 0.2$ (blue) and of the heteroclinic orbits in the system without feedback at $\kappa = 0$ (purple). (b) – Enlargement of framed region in (a) close to the background equilibrium. (c) – time traces of the soliton and of the feedback-term. Parameters: $V_4 = 0.13$, other parameters as in Fig. 1.

Due to the excitability of the stable equilibrium already a small input from the feedback term can lead to an excitation pulse. In this way the feedback can induce periodic solutions, where each of the subsequent pulses is triggered by the previous pulse entering the feedback term. Figure 5(a) displays the heteroclinc orbits for the ODE (purple trajectories) together with a soliton periodic orbit of the DDE (blue). While both trajectories behave more or less similar for most of the time, the zoom in panel (b) shows that close to the equilibrium, the ODE and DDE trajectories point in almost opposite directions. This is exactly the moment, when the feedback term I_{ext} is not close to zero (cf. panel (c)).

Note that this mechanism works for any large enough value of the delay τ, such that one can use the limit $\tau \to \infty$ for an approximation of the case of large but finite values of the delay. In fact, TDSs can be characterized by the fact that they appear as families of periodic orbits parametrized by the delay parameter τ with corresponding periods $T(\tau)$ and a *response time*

$$\delta_\tau := T(\tau) - \tau$$

which is always positive and tends to a finite limit δ_∞ when $\tau \to \infty$.

In [45] it has been pointed out that the profile of a soliton can be calculated not only as a periodic solution of the DDE with large delay τ, but also for τ replaced by $-\delta_\tau$. This is due to the general fact that any T-periodic solution of a DDE with delay τ_0 reappears as a solution for all

$$\tau_k = \tau_0 + kT, \quad k \in \mathbb{Z}, \tag{6}$$

see [44]. In this case, this allows us to replace the singular limit $\tau \to \infty$ with the regular situation $\delta \to \delta_\infty$. At this value, the profile of TDS is given as a homoclinic orbit tending for $t \to \pm\infty$ to the background equilibrium. Replacing the delay time τ by $-\delta$ the original delay equation turns into an equation with advanced argument, which is called *profile equation*. For such equations initial value problems can be solved only backward in time. Note that the the reappearing periodic solutions, as well as the equilibria, which are also preserved when the delay time is changed, have different stability properties. The background equilibrium is assumed to be stable for all large positive values of the delay τ. Hence, according to [46] it is absolutely stable, i.e. stable for all positive τ. However, in the profile equation it turns into an equilibrium of saddle type such that a homoclinic orbit approaching this equilibrium can appear.

Recall that in generic dissipative systems homoclinic orbits are of codimension one, i.e in order to obtain a homoclinic solution one typically has to adjust one parameter. Thus, we can solve the profile equation simultaneously for a homoclinic solution, giving the profile of the TDS, and for the asymtotic response time δ_∞. At the same time, soliton periodic orbits are generic solutions of the DDE with large delay. They persist for small changes of the parameters and can be found for all sufficiently large values of the delay. Hence, our codimension-one homoclinic solution from the profile equation corresponds to a generic soliton solution of the original system, where δ is not a control parameter, but is already determined by the soliton. In all bifurcation problems for the profile equation, this specific role of δ leads to the fact that codimension-two homoclinic phenomena in the profile equation refer to codimension-one situations for the solitons in the original DDE with large delay.

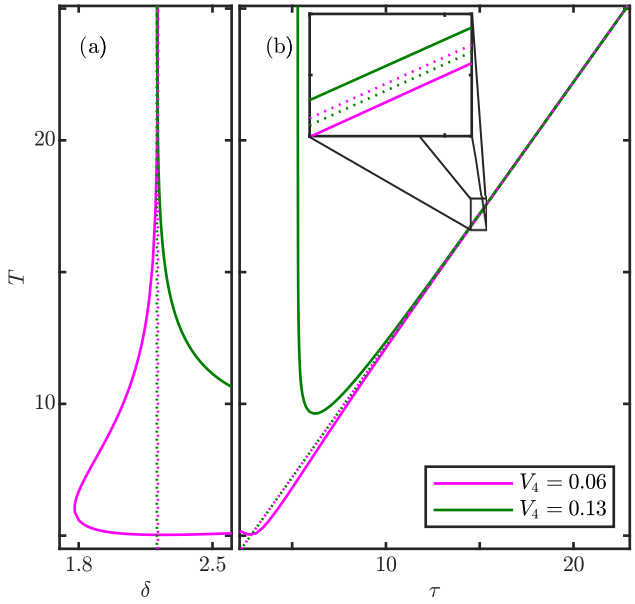

FIGURE 6. Branches of periodic solutions in the profile equation (a) and in the large delay DDE (b) for two different choices of V_4. In the DDE (b), the branches approach the lines $\tau + \delta_\infty$ (dashed), while both T and τ become infinite. In the profile equation each branch approaches a vertical line at $\delta = \delta_\infty$ with $T \longrightarrow \infty$ in a homoclinc bifurcation. Other parameters as in Fig. 1.

Figure 6 illustrates the relation between the original DDE with large delay and the profile equation. Panel (b) shows the typical signature of a TDS: a branch of periodic solutions that exists for all large τ, while its period T approaches the line $T = \tau + \delta_\infty$ (dashed lines). In panel (a) the same branches of periodic orbits are shown, now as periodic solutions of the profile equation. The period increases when δ approaches δ_∞, displaying a classical homoclinic bifurcation while all system parameters remain bounded. The homoclinic orbit approaches the background equilibrium, which in the profile equation is always a saddle. Note that for the original DDE with large delay the soliton orbit actually comes never close to the background equilibrium in terms of the infinite dimensional phase space since there is always a pulse contained in the history interval.

The two soliton branches in Fig. 6 correspond to the profiles shown in Fig. 1(a) and represent the two different regimes of the Morris–Lecar model without feedback, shown in Fig. 3 in purple and blue, respectively. They differ by the undershoot in V (hyperpolarization), which is not present in the purple region. This different shape of the trajectory comes together with a qualitative difference in the response time δ_τ. In the purple region, the response time for finite τ is smaller than its asymptotic value δ_∞, while in the blue region it is bigger. We will show in the next section how this difference is related to the different behavior of the multi-pulse solutions shown in Fig. 1 and Fig. 2.

Using the profile equation, one can use standard methods to study existence and bifurcations of TDSs, see also [11]. Note that in order to use DDEbiftool for a system with an advanced argument, the time has to be reversed. In Fig. 7 we show the parameter region of stable solitons in the (E_l, V_4)-parameter plane in the neighbourhood of the SNSL point. For our choice of $\kappa = 0.2$ stable TDSs exist only up to a certain distance from the saddle-node curve. This can be explained by the fact that at larger distance from the saddle-node also the excitation threshold becomes higher such that at a certain point the given feedback strength is no more sufficient to sustain the generation of subsequent pulses. This stability boundary is given as a subcritical period-doubling (green curve in Fig. 7) of the soliton periodic solutions. In contrast to the other bifurcations in this diagram, this type of period doubling cannot be calculated in the framework of the profile equation, see [11], Lemma 1. We used instead a continuation based on soliton periodic orbits of the original large delay DDE.

Remarkably, the other stability boundaries are closely related to the bifurcations from the Morris–Lecar model without feedback, described in section 1. In Fig. 7 they are given by black lines. Close to the homoclinic bifurcation of the Morris–Lecar model without feedback (black dashed line) there is the stability boundary of the solitons. Close to the SNSL point, it is given as a curve of Bykov T-points [4, 19] (red curve). Approaching this curve, the soliton profile approaches also the unstable saddle equilibrium and in this way becomes itself unstable. The curve of Bykov T-points has been calculated in the framework of the profile equation by a continuation of a codimension-two heteroclinic between the saddle equilibrium and the original background equilibrium of the soltion; for details of the method see [29, 1]. Using in the continuation also the asymptotic response time δ_∞ as a free parameter, we obtain a codimension-one curve in the original system parameters.

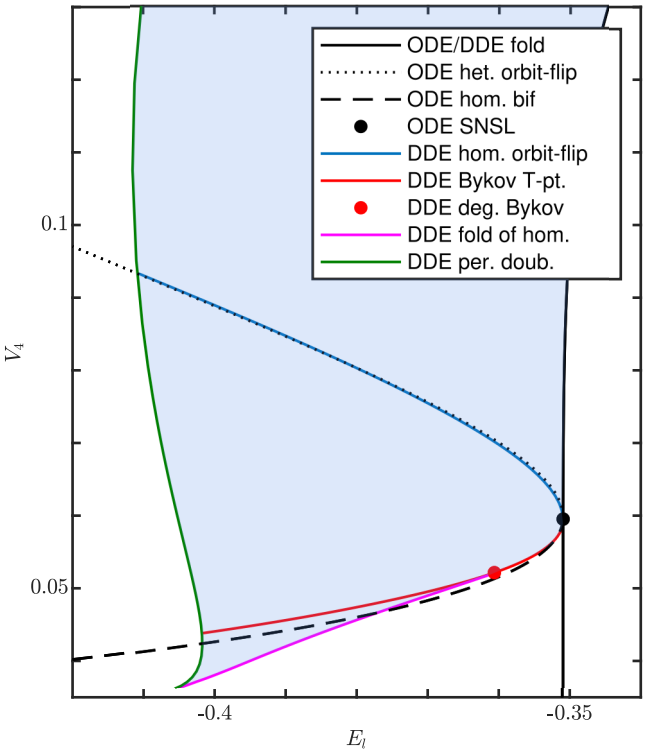

FIGURE 7. Stability region (blue) and bifurcation curves (coloured) of the single pulse soliton in the DDE system $\kappa = 0.2$ and bifurcations of the ODE system $\kappa = 0$ (black) with SNSL point in the (E_l, V_4)-parameter plane, cf schematic picture in Fig. 3. Other parameters as in Fig. 1.

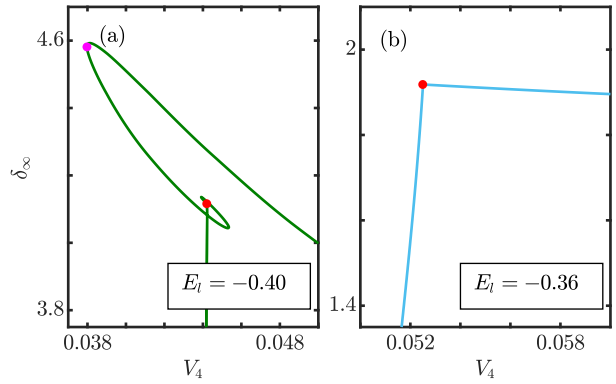

FIGURE 8. Branches of single pulse solutions for varying parameter V_4. (a) – For $E_l = -0.4$, unfolding of Bykov T-point (red dot) with the saddle equilibrium of saddle focus type and fold point (magenta). (b) – For $E_l = -0.36$ Bykov T-point (red dot) with simple saddle. Other parameters as in Fig. 1.

At the red point located on this branch in Fig. 7, the saddle equilibrium has a double eigenvalue in the linearized profile equation and changes from a simple saddle (two real leading eigenvalues) to a saddle focus (one complex conjugate pair and one real leading eigenvalue). Qualitatively, this changes the unfolding of the T-point, see Fig. 8: In the case of real leading eigenvalues, the branch of homoclinics displays a kink at the T-point, see panel (b). In the case where the saddle equilibrium is of saddle-focus type, the branch has a spiraling shape and undergoes a sequence of folds (see panel (a)) before hitting the T-point in the center of the spiral. Hence, beyond this degenerate Bykov T-point the stability boundary of the soliton is given by a fold of solitons (magenta curve in Fig. 7). Along this fold curve, the manifold of homoclinic solutions of the profile equation is folded with respect to the parameter δ_∞.

In the interior of the stability region there is the heteroclinic orbit flip (black dotted line) of the system without feedback. It is accompanied by a homoclinic orbit flip of the system with feedback (blue curve), which is computed by a continuation of a connecting orbit with the corresponding asymptotic behavior in the profile equation.

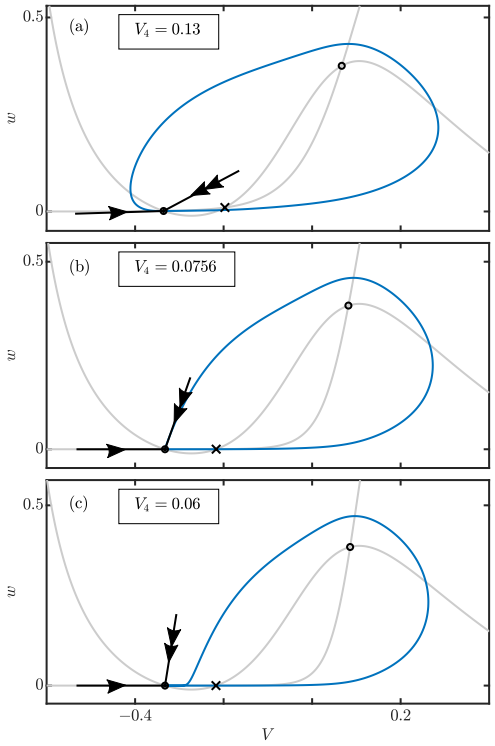

FIGURE 9. Homoclinic orbit flip in the profile equation. The different choices of parameter V_4 in panels (a)–(c) represent the situation before, directly at, and after the orbit flip, respectivley. Stable, saddle and unstable equilibrium are indicated by black dot, cross, and circle, respectively. Projection of leading stable eigendirection of stable equilibrium indicated with single arrow, of strong stable eigendirection indicated with double arrow. Other parameters as in Fig. 1.

3. HOMOCLINIC ORBIT FLIP INDUCES PULSE PACKAGES

Figure 9 depicts the phase portraits of the homoclinics before the flip (panel (a)), directly at the flip, when the homoclinic passes through the strong stable eigendirection of the equilibrium (b), and after the flip, when the homoclinic orbit approaches its saddle again along the corresponding leading eigendirection, but now from the other side (c). The corresponding stable eigendirections, indicated by the black arrows, are the eigenfunctions of the linear delay operator, projected to the (V, w)-plane. For $t \to -\infty$ the homoclinic approaches the equilibrium along an unstable eigenfunction, which cannot be shown properly in this projection.

In contrast to the heteroclinc orbit flip, shown for the ODE without feedback in Fig. 4, the homoclinic orbit flip is a codimension-two phenomenon [30] and for its continuation as a DDE connecting orbit (blue curve in Fig. 7) we have to use the parameters V_4, E_l, and δ. Recall that the corresponding branches of periodic orbits for panel (a) and (c) have been shown in Fig. 6. Note that the branch corresponding to $V_4 = 0.06$ (magenta in panel (a)) has a fold of limit cycles. At the homoclinic orbit flip, this fold collides with the homoclinic bifurcation and disappears. Indeed, according to general homoclinic bifurcation theory, see e.g. the review by Homburg & Sandstede [15] and references therein, there can be additional codimension-1 bifurcations, emanating from a homoclinic orbit flip. In the situation given here, the orbit flip generates infinitely many branches of N-homoclincs. They come together with a period doubling and resonant Neimark-Sacker bifurcations of the accompanying periodic orbits with large period, which are relevant for the multi-pulse solutions, shown in Fig. 1. Applying the reappearance rule (6) with $k > 1$ to the soliton solution with a single pulse ($k = 1$), we obtain multi-pulse solutions with several equidistant pulses within one delay interval. For these solutions each pulse is not triggered by the directly preceding pulse, but by the k-th preceding pulse, which in this case has the distance close to τ. Note that for a stable soliton, the corresponding equidistant multi-pulse solutions can be stable or unstable, in particular depending on the stability with respect to their relative distance. At the other hand, the N-homoclincs in the profile equation, correspond to soliton solutions with a single localized pulse package and can formally be treated analogously to single-pulse solitons.

In Fig. 10 we show branches of multi-pulse solutions obtained from numerical continuations with varying parameter V_4, crossing the orbit flip bifurcation. The stability of the branch of single pulse solutions is not affected by the orbit flip. As we have already demonstrated in Fig. 1, in the parameter region above the orbit flip (blue region in Fig. 3) the equidistant

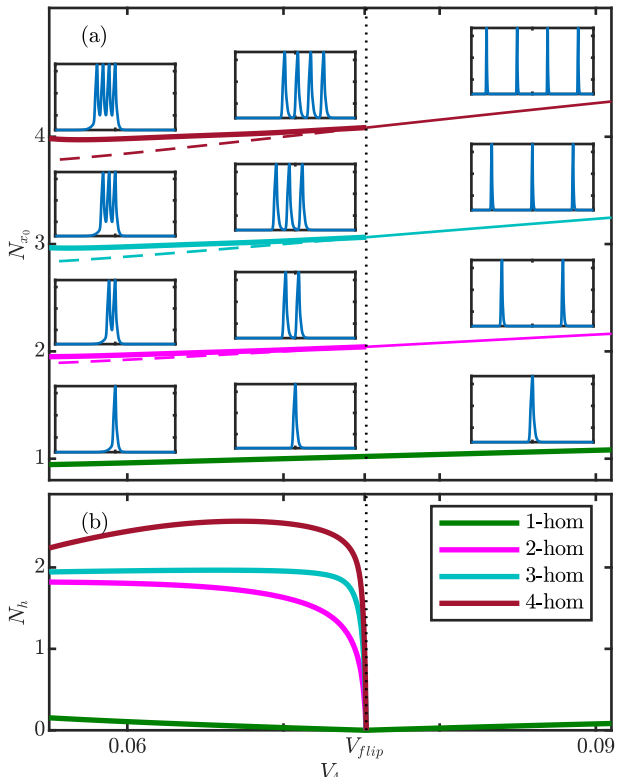

FIGURE 10. Homoclinic orbit flip along the branch of single pulse solitons (green curves) induces bifurcations along the branches of multi-pulse solutions (curves of other colours). For $V_4 > V_{flip}$ the equidistant multi-pulse solutions are stable. For $V_4 < V_{flip}$ the equidistant multi-pulse solutions are unstable (dashed curves) and stable non-equidistant multi-pulse solutions bifurcate (solid curves). Along the branch they turn into pulse packages with decreasing spacing of the pulses (see insets). The quantities N_{x_0} and N_h, used in panels (a) and (b) are given in (7) and (8), respectively. Other parameters as in Fig. 1.

multi-pulse solutions turn out to be stable. Directly at the orbit flip they lose their stability and branches of stable non-equidistant multi-pulse solutions bifurcate. For the double pulse, this is a period doubling bifurcation, while it is a resonant Neimark-Sacker bifurcation for $k > 2$. Along the branch, these pulse packages are getting packed more and more closely, see insets in Fig. 10. In panels (a) and (b), we used two different distance measures to display the branches. With

$$N_{x_0} = ||h - x_0||^2_{L^2} \tag{7}$$

we measure the L^2-distance of a solution profile h to the background equilibrium x_0. In this way, each k-pulse solution appears as a different branch and also the increasing distance between the unstable equidistant pulses (dashed) and the corresponding stable pulse package becomes visible. In panel (b) we use instead the distance

$$N_h = ||h - h_{V_{flip}}||_{L^2}, \tag{8}$$

of a solution profile h to the corresponding profile with k equidistant pulses from the orbit flip. This shows that, for large delay, when becoming equidistant, the shapes of all pulses for all different k become equal and all k-pulse packages bifurcate at the critical value at $V_4 = V_{flip}$ from the profile corresponding to the degenerate homoclinic. all together, this implies the coexistence of stable equidistant k-solitons for $V_4 > V_{flip}$ and stable k-pulse packages for $V_4 < V_{flip}$ in the large delay DDE.

For large but finite values of the delay τ the infinite number of bifurcating N-homoclinic solutions, predicted by the homoclinic theory, turns into a finite number of multi-pulse solutions up to the possible number of pulses that can be accommodated within the delay interval. A similiar scenario of multi-pulse solutions where the number of pulses gradually increases with increasing delay has been presented in a detailed bifurcation analysis of the Yamada model with delayed feedback [38, 39]. Treating the delay as the main bifurcation parameter and using classical numerical bifurcation analysis, their approach is restricted to moderate values of τ and gives a detailed picture of the effects caused by the finite delay and the changing number of admissible pulses for varying delay.

4. Conclusion

We demonstrated how complicated dynamics of TDSs in systems with time delay can be analyzed in the framework of the profile equation by means of homoclinic bifurcation theory. The approach via the profile equation is similar to the ßpatial dynamicsäpproach, which has been widely used to study pulse and also wave solutions in spatially extended systems, see e.g. Ref. [18], and adds a new chapter to the relationship between delayed and spatially extended systems [10]. The profile equation is of advanced type, which resembles the causality within the original large delay DDE, and the finite advanced time shift removes the singular nature of the limit of large delay. This equation is also extremely useful for the numerical treatment and bifurcation analysis, which can become numerically difficult in the original systems with the large delay. Note that not only the homoclinics, calculated in this way, can serve as approximations of the soliton solutions and reproduce the bifurcation structure. In fact, the large period periodic orbits that come along with the homoclinics in the profile equation exactly reproduce soliton solutions for large but finite delay. As in the case of the spatial dynamics, the stability properties of solutions with respect to the linearized profile equation are different from those of the soliton in the linearized original large delay DDE. The relation between specific homoclinic bifurcations and the corresponding bifurcations and instabilities of the TDSs is not straight forward. In particular, the specific role of the response time δ as an additional parameter in the profile equation has to be considered carefully.

The scenario of a homoclinic orbit flip, which we studied here in detail, leads to pulse packages, sometimes also called "bound states", without oscillatory tails of the profiles. The coexistence of such stable pulse packages with an increasing number of pulses reminds of the homoclinic snaking scenario, which has been studied extensively in the context of spatially extended systems [3]. Here, however, the pulse packages are not organized on a single snaking branch where pulses are added in the course of subsequent foldings. Instead, the stable pulse packages emerge from equidistant pulses at the homoclinic orbit flip and disappear by the collision of their profile with another unstable equilibrium in a Bykov T-point, which induces a destabilization. Beyond this stability boundary, we observe that the pulse package solutions display a trailing edge instability that induces the subsequent generation of additional pulses until a uniformly pulsating solution is reached, see Fig. 2 (b).

It turns out that for small feedback strength, the bifurcations leading to different types of excitability in the Morris–Lecar model, can be directly related to the dynamics of the solitons and multi-pulse solutions. For larger feedback strength or feedback including also the activation variable w one might expect other and more complicated dynamical scenarios.

References

[1] W.-J. Beyn. The numerical computation of connecting orbits in dynamical systems. IMA Journal of Numerical Analysis, 10(3):379–405, 07 1990.

[2] A. Borisyuk and J. Rinzel. Understanding neuronal dynamics by geometrical dissection of minimal models. Methods and Models in Neurophysics (1st Ed., Elsevier, 2005), pages 17–72, 2005.

[3] J. Burke and E. Knobloch. Homoclinic snaking: Structure and stability. Chaos: An Interdisciplinary Journal of Nonlinear Science, 17(3):037102, 2007.

[4] V. V. Bykov. The bifurcations of separatrix contours and chaos. Physica D, 62(1–4):290–299, Jan 1993.

[5] S.-N. Chow and X.-B. Lin. Bifurcation of a homoclinic orbit with a saddle-node equilibrium. Differential Integral Equations, 3:435–466, 1990.

[6] B. Deng. Homoclinic bifurcations with nonhyperbolic equilibria. SIAM Journal on Mathematical Analysis, 21(3):693–720, 1990.

[7] L. Duan, D. Zhai, and Q. Lu. Bifurcation and bursting in Morris-Lecar model for class I and class II excitability. Discrete and Continuous Dynamical Systems- Series A, 09 2011.

[8] G. B. Ermentrout and D. H. Terman. Mathematical foundations of neuroscience. Interdisciplinary Applied Mathematics, 2010.

[9] B. Garbin, J. Javaloyes, G. Tissoni, and S. Barland. Topological solitons as addressable phase bits in a driven laser. Nature Communications, 6(1):1–7, 2015.

[10] G. Giacomelli and A. Politi. Relationship between delayed and spatially extended dynamical systems. Phys. Rev. Lett., 76:2686–2689, Apr 1996.

[11] A. Giraldo and S. Ruschel. Pulse-adding of temporal dissipative solitons: Resonant homoclinic points and the orbit flip of case B with delay, 2022.

[12] F. Gustave, L. Columbo, G. Tissoni, M. Brambilla, F. Prati, B. Kelleher, B. Tykalewicz, and S. Barland. Dissipative phase solitons in semiconductor lasers. Physical Review Letters, 115(4):043902, 2015.

[13] S. Heiligenthal, T. Dahms, S. Yanchuk, T. Jüngling, V. Flunkert, I. Kanter, E. Schöll, and W. Kinzel. Strong and weak chaos in nonlinear networks with time-delayed couplings. Phys. Rev. Lett., 107:234102, Nov 2011.

[14] D. Hessel, S. V. Gurevich, and J. Javaloyes. Wiggling instabilities of temporal localized states in passively mode-locked vertical external-cavity surface-emitting lasers. Optics Letters, 46(10):2557–2560, 2021.

[15] A. J. Homburg and B. Sandstede. Homoclinic and heteroclinic bifurcations in vector fields. In H. Broer, B. Hasselblatt, and F. Takens, editors, Handbook of Dynamical Systems, volume 3, chapter 8, pages 379–524. North-Holland, Elsevier Science, 2010.

[16] E. Izhikevich. Neural excitability, spiking and bursting. Int. J. Bifurc. Chaos, 10:1171–1266, 2000.

[17] E. M. Izhikevich. Dynamical Systems in Neuroscience: The Geometry of Excitability and Bursting. The MIT Press, 2007.

[18] K. Kirchgässner. Nonlinearly resonant surface waves and homoclinic bifurcation. Advances in Applied Mechanics, 26:135–181, 1988.

[19] J. Knobloch, J. S. Lamb, and K. N. Webster. Using lin's method to solve bykov's problems. Journal of Differential Equations, 257(8):2984–3047, 2014.

[20] M. Lichtner, M. Wolfrum, and S. Yanchuk. The spectrum of delay differential equations with large delay. SIAM J. Math. Anal., 43:788–802, 2011.

[21] B. Lindner, J. García-Ojalvo, A. Neiman, and L. Schimansky-Geier. Effects of noise in excitable systems. Physics Reports, 392(6):321–424, 2004.

[22] C. Liu, X. Liu, and S. Liu. Bifurcation analysis of a morris–lecar neuron model. Biological Cybernetics, 108:75–84, 2013.

[23] M. Marconi, J. Javaloyes, S. Balle, and M. Giudici. How lasing localized structures evolve out of passive mode locking. Phys. Rev. Lett., 112:223901, Jun 2014.
[24] C. Morris and H. Lecar. Voltage oscillations in the barnacle giant muscle fiber. Biophysical Journal, 35(1):193–213, 1981.
[25] L. Munsberg, J. Javaloyes, and S. V. Gurevich. Topological localized states in the time delayed adler model: Bifurcation analysis and interaction law. Chaos: An Interdisciplinary Journal of Nonlinear Science, 30(6):063137, Jun 2020.
[26] M. Nizette, D. Rachinskii, A. Vladimirov, and M. Wolfrum. Pulse interaction via gain and loss dynamics in passive mode locking. Physica D: Nonlinear Phenomena, 218(1):95–104, 2006.
[27] J. Rinzel and G. Ermentrout. Analysis of neural excitability and oscillations. In C. Koch and I. Segev, editors, Methods in neuronal modeling, chapter 7, pages 251–291. MIT Press, 2 edition, 1998.
[28] S. Ruschel, B. Krauskopf, and N. G. R. Broderick. The limits of sustained self-excitation and stable periodic pulse trains in the yamada model with delayed optical feedback. Chaos: An Interdisciplinary Journal of Nonlinear Science, 30(9):093101, 2020.
[29] G. Samaey, K. Engelborghs, and D. Roose. Numerical computation of connecting orbits in delay differential equations. Numerical Algorithms, 30(3):335–352, Aug 2002.
[30] B. Sandstede. Verzweigungstheorie homokliner Verdopplungen. WIAS Report, 7, 1993.
[31] S. Schecter. The saddle-node separatrix-loop bifurcation. SIAM J. Math. Anla., 18:1142–1157, 07 1987.
[32] C. Schelte, P. Camelin, M. Marconi, A. Garnache, G. Huyet, G. Beaudoin, I. Sagnes, M. Giudici, J. Javaloyes, and S. V. Gurevich. Third order dispersion in time-delayed systems. Phys. Rev. Lett., 123:043902, Jul 2019.
[33] C. Schelte, J. Javaloyes, and S. V. Gurevich. Dynamics of temporally localized states in passively mode-locked semiconductor lasers. Phys. Rev. A, 97:053820, May 2018.
[34] C. Schelte, A. Pimenov, A. Vladimirov, J. Javaloyes, and S. Gurevich. Tunable kerr frequency combs and temporal localized states in time-delayed gires–tournois interferometers. Optics Letters, 44:4925, 10 2019.
[35] L. P. Shilnikov, A. L. Shilnikov, D. V. Turaev, and L. O. Chua. Methods of Qualitative Theory in Nonlinear Dynamics - Part II, volume 5. World Scientific, 2001.
[36] J. Sieber, K. Engelborghs, T. Luzyanina, G. Samaey, and D. Roose. Dde-biftool manual - bifurcation analysis of delay differential equations. arXiv: Dynamical Systems, 2016.
[37] J. Sieber, M. Wolfrum, M. Lichtner, and S. Yanchuk. On the stability of periodic orbits in delay equations with large delay. Discrete and Continuous Dynamical Systems, 33(7):3109–3134, 2013.
[38] S. Terrien, B. Krauskopf, and N. G. Broderick. Bifurcation analysis of the Yamada model for a pulsing semiconductor laser with saturable absorber and delayed optical feedback. SIAM Journal on Applied Dynamical Systems, 16(2):771–801, 2017.
[39] S. Terrien, V. A. Pammi, B. Krauskopf, N. G. R. Broderick, and S. Barbay. Pulse-timing symmetry breaking in an excitable optical system with delay. Phys. Rev. E, 103:012210, Jan 2021.
[40] K. Tsumoto, H. Kitajima, T. Yoshinaga, K. Aihara, and H. Kawakami. Bifurcations in morris–lecar neuron model. Neurocomputing, 69:293–316, 01 2006.
[41] A. G. Vladimirov. Short- and long-range temporal cavity soliton interaction in delay models of mode-locked lasers. Physical Review E, 105, 04 2022.
[42] A. G. Vladimirov and D. Turaev. Model for passive mode locking in semiconductor lasers. Physical Review A, 72(3):033808, 2005.
[43] S. Yanchuk and G. Giacomelli. Spatio-temporal phenomena in complex systems with time delays. Journal of Physics A: Mathematical and Theoretical, 50:103001, 03 2017.
[44] S. Yanchuk and P. Perlikowski. Delay and periodicity. Phys. Rev. E, 79:046221, Apr 2009.
[45] S. Yanchuk, S. Ruschel, J. Sieber, and M. Wolfrum. Temporal dissipative solitons in time-delay feedback systems. Phys. Rev. Lett., 123:053901, Jul 2019.
[46] S. Yanchuk, M. Wolfrum, T. Pereira, and D. Turaev. Absolute stability and absolute hyperbolicity in systems with discrete time-delays. Journal of Differential Equations, 318:323–343, 2022.